Heliyon 10 (2024) e33097

Contents lists available at ScienceDirect

Heliyon

journal homepage: www.cell.com/heliyon

Research article

Moss biomass as effective biosorbents for heavy metals in contaminated water

Chetsada Phaenark [a], Sarunya Nasuansujit [a], Natdanai Somprasong [b], Weerachon Sawangproh [a,*]

[a] Conservation Biology Program, School of Interdisciplinary Studies, Mahidol University, (Kanchanaburi Campus), 199 Moo 9 Lumsum, Sai Yok District, Kanchanaburi 71150, Thailand

[b] Division of Research, Innovation, and Academic Services, Mahidol University, (Kanchanaburi Campus), 199 Moo 9 Lumsum, Sai Yok District, Kanchanaburi 71150, Thailand

ARTICLE INFO

Keywords:
Biosorption
Sustainable
Environmentally friendly
Pottiaceae
Remediation

ABSTRACT

The study explored batch adsorption of Cd(II) and Pb(II) ions using moss biomass from *Barbula consanguinea* and *Hyophila involuta*, assessing removal efficiency concerning various parameters. Both moss species showed high removal rates for Cd(II) (87 % for *B. consanguinea* and 89 % for *H. involuta*) and Pb(II) (93 % for *B. consanguinea* and 94 % for *H. involuta*) from contaminated water, reaching equilibrium within 30 min. While Cd(II) removal was pH-independent, Pb(II) removal showed pH-dependence, peaking at pH 5.0–5.5. Adsorption isotherm analysis indicated that the Langmuir, Freundlich, Elovich, Sips, and Redlich-Peterson models best described Cd(II) and Pb(II) adsorption onto both moss species (except for Cd(II) adsorption onto *H. involuta*), with $R^2 > 0.98$. This confirms a heterogeneous surface with both monolayer and multilayer adsorption sites. The pseudo-second-order kinetic model confirmed chemisorption on moss biomass from both species. FTIR spectra identified major binding sites such as phenols, alkaloids, amines, alkenes, nitro compounds, and low-molecular-weight carbohydrates. EDS analysis validated the bonding of Cd(II) and Pb(II) ions to the biomass surface by displacing Ca(II) ions. According to the Langmuir model, moss biomass exhibited selective adsorption, favoring Pb(II) over Cd(II). *B. consanguinea* showed a higher adsorption capacity than *H. involuta*, which is attributed to its higher negative zeta potential. This study underscores the novelty of moss biomass for heavy metal removal in wastewater treatment, highlighting its sustainability, effectiveness, cost-efficiency, versatility, and eco-friendliness.

1. Introduction

Heavy metal contamination in water resources has emerged as a critical environmental concern due to the profound impact it has on ecosystems and human health [1]. Among the myriad heavy metals, cadmium (Cd) and lead (Pb) stand out as particularly troublesome, given their inherent toxicity and persistence in aquatic environments [2]. Extensive research on the harmful impacts of Cd and Pb contamination has been conducted for years in developed nations. However, this issue is often overlooked in most developing countries [3]. Thailand, like many others, faces significant Cd and Pb pollution in areas associated with past mining activities. For

* Corresponding author.
E-mail address: weerachon.saw@mahidol.edu (W. Sawangproh).

https://doi.org/10.1016/j.heliyon.2024.e33097
Received 22 March 2024; Received in revised form 13 May 2024; Accepted 22 May 2024
Available online 17 June 2024

example, Cd contamination in Mae Sot District (Tak Province) and Pb contamination in Klity Creek (Kanchanaburi Province) are prevalent [4]. Cd and Pb are known for their adverse effects on living organisms, even at trace concentrations [5,6]. Human exposure to these metals can lead to severe health issues, including neurological disorders, developmental abnormalities, and organ damage [7]. Additionally, the persistent nature of Cd and Pb in water systems raises long-term environmental challenges, as these metals can accumulate in sediments and biota, posing a continuous threat to the ecosystem [8].

The recognition of these hazards has spurred extensive research into effective remediation strategies to mitigate the impact of heavy metal contamination. Consequently, exploring sustainable and natural methods for removing these heavy metals from water resources has become imperative to safeguard both the environment and public health [9]. Utilising dried biomass as a bio-based adsorbent for heavy metal adsorption offers a sustainable solution for environmental remediation [9]. Dried biomass, derived from various sources such as agricultural residues [10], microbes such as fungi, bacteria, and algae [11], natural waste adsorbent including clay, zeolite, chitosan, peat and siliceous material [9], or activated sludge [12], possesses inherent properties that make it an effective adsorbent for heavy metals. The porous structure and high surface area of dried biomass provide ample binding sites for heavy metal ions [13], facilitating their removal from aqueous solutions through adsorption processes. Moreover, the abundance and renewability of biomass make it a cost-effective and environmentally friendly alternative to conventional adsorbents [14]. Through proper pre-treatment and modification techniques, the adsorption capacity and selectivity of dried biomass can be enhanced, optimising its performance in heavy metal removal applications [15].

Bryophytes, which encompass mosses, liverworts, and hornworts, demonstrate notable proficiency in absorbing heavy metals, rendering them invaluable as biomonitors and bioindicators [16,17]. Mosses, in particular, excel at absorbing and accumulating hazardous substances, including potentially toxic elements (PTEs), often exceeding their physiological requirements [18], especially in polluted streams and urban areas [19]. The absence of roots [20] and the lack of a waxy cuticle layer on their leaf surfaces [21], which aids in pollutant absorption, enable them to directly absorb pollutants into their cells from the air rather than from substrates [20]. In terms of environmental cleanup, mosses possess key attributes that make them particularly suitable for heavy metal adsorption, with molecules of pollutants adhering to their surface. Such attributes include an exceptionally high surface-to-volume ratio, the high stability of devitalised mosses in aqueous solutions, low production costs for natural or artificially grown specimens [22], and ion-exchange capacity [18].

The intricate network of leaves, stems, and rhizoids in mosses provides an extensive interface for contact with aqueous solutions, facilitating increased opportunities for the adsorption of metal ions. This enhanced surface area is pivotal in maximising the efficiency of mosses as biosorbents [23] in capturing and immobilising heavy metals from contaminated water sources. Furthermore, the abundant functional groups present in moss tissues play a crucial role in their metal-binding capabilities [23]. The functional groups on the surfaces of mosses possess a strong affinity for metal ions, allowing for the complexation and chelation of heavy metals [24]. This inherent capacity to form bonds with metals makes mosses effective natural adsorbents, capable of removing a wide range of heavy metal pollutants from aqueous solutions [25]. Additionally, the robustness and adaptability of mosses in diverse environmental conditions [26] make them resilient candidates for biosorption applications. For example, by incorporating moss biomass into composite adsorbents, synergistic effects may be achieved, leading to enhanced adsorption efficiency and selectivity. The customisation potential of composite adsorbents allows for the optimisation of adsorption properties to suit specific wastewater conditions and target pollutants [27–30].

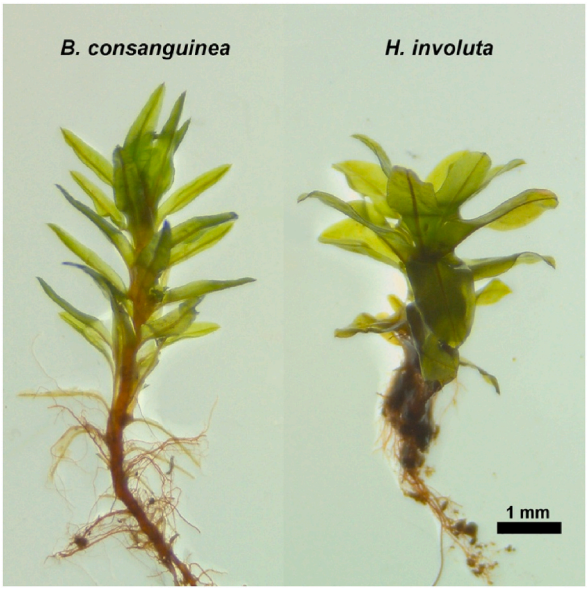

Fig. 1. Two acrocarpous mosses used for preparing biosorbent.

In this study, we prioritise cadmium (Cd) and lead (Pb) metals because they are toxic to humans [31], commonly used in any industrial, urban, or agricultural applications [32], and found together as contaminants in the environment [33], with the aim of achieving several objectives. Firstly, we sought to quantify the ability of biosorbents derived from the mosses *Barbula consanguinea* and *Hyophila involuta* to adsorb Cd(II) and Pb(II) ions from single-metal systems. Secondly, we aimed to compare the affinity of the biosorbents for these ions in single-metal systems prepared from *B. consanguinea* and *H. involuta*. Thirdly, we aimed to investigate the uptake of Cd(II) and Pb(II) ions onto moss dried biomass using various adsorption isotherm models, as not all isotherms can fit the experimental data and describe the heavy metal adsorption process [34]. We also aimed to evaluate adsorption kinetics through batch adsorption experiments. Additionally, we endeavoured to characterise the functional groups of the moss biosorbents using FTIR analysis and study the metal biosorption mechanism using scanning electron microscopy connected with EDX analysis. Given mounting concerns regarding heavy metal contamination in water resources, especially the persistent and hazardous nature of Cd and Pb, our research addresses the urgent need for environmentally sound remediation solutions. The selection of moss biomass as a natural adsorbent aligns with the increasing demand for sustainable alternatives, underscoring the potential of readily available and biodegradable materials in combating waterborne pollutants. By elucidating the adsorption kinetics and mechanisms involved in the interaction between moss biomass and Cd(II) and Pb(II) ions, our study aims to offer valuable insights into the development of practical, cost-effective, and sustainable approaches for water treatment. Ultimately, our research contributes to advancing the understanding of green technologies for heavy metal remediation, advocating for a paradigm shift towards more ecologically conscious water management practices.

2. Materials and methods

2.1. Biomass preparation

Acrocarpous mosses *Barbular consanguinea* (Thwaites & Mitt.) A.Jaeger and *Hyophila involuta* (Hook.) A.Jaeger (Fig. 1) were gathered between August and December 2022 from specific locations at Mahidol University (Kanchanaburi Campus) in Kanchanaburi Province, Thailand. The collection sites comprised a nursery greenhouse (14.129719° N, 99.158970° E) for *H. involuta* and soil adjacent to a horse stable (14.136229° N, 99.149067° E) for *B. consanguinea*. The collected moss materials were thoroughly washed with distilled water, repeating the process 3–4 times before use. Only fresh leaves and stems of gametophores were used. Following collection, the plants underwent cutting into small pieces and were dried in an oven at 50–60 °C for approximately 5–7 days. After drying, the plants were finely ground using a blender (PHILIPS, model HR 2115) and sifted through a 250-μm sieve. The resulting biomass powder was stored in a zip-lock plastic bag and kept in a desiccant jar for subsequent studies.

2.2. Characterisation of moss biomass

Prior to heavy metal adsorption, we conducted measurements of the Brunauer-Emmett-Teller (BET) surface area, the Barrett-Joyner-Halenda (BJH) pore size distribution, and total pore volume (using the t-plot method) for 0.0454 g of *B. consanguinea* biomass and 0.0507 g of *H. involuta*. These measurements were carried out using a Quantachrome® ASiQwinTM system. Vacuum degassing was performed at 80 °C for 15.2 h and held at this temperature for 5 h and 44 min for *B. consanguinea*, and for 5 h and 52 min for *H. involuta*.

To assess the net surface charge of the biomass, reflecting a balance between positive and negative surface sites [35], we measured the zeta potential of native moss biomass at 25 °C. This involved dispersing the moss biomass in deionized water using a Zeta-sizer (Nano ZSP, Malvern Instruments Ltd.), with three measurement replicates conducted for reliable data. In terms of heavy metal adsorption, biomass materials with a high negative zeta potential are typically preferred. They can attract and bind positively charged heavy metal ions through electrostatic attraction.

2.3. Heavy metal aqueous solution preparation

The chemical preparation process involved creating single-metal solution systems containing either Pb(II) ions or Cd(II) ions. These solutions were prepared in Erlenmeyer flasks by dissolving $Pb(NO_3)_2$ (molecular weight: 331.20) to create a 1000 mg Pb/L stock solution and $CdCl_2{\cdot}2.5H_2O$ (molecular weight: 228.35) to form a 1000 mg Cd/L stock solution. Each concentration (5, 10, 15, 30, 50, 70, and 90 mg/L for Pb and Cd) was prepared in triplicate. The pH of each solution was adjusted from 5.0 to 7.0 by adding 1 M HNO_3 (Merck) and NaOH (Merck).

2.4. Adsorption studies in single-metal systems

All adsorption experiments were conducted on a rotary shaker at 120 rpm using 250 mL Erlenmeyer flasks and carried out at room temperature (25 °C). The first experiment aimed to investigate the effect of adsorbent contact and equilibrium time. For this purpose, Cd(II) solution (50 mL, 50 mg/L) or Pb(II) solution (50 mL, 90 mg/L) along with 0.10 g of moss biomass (0.2 % w/v) were added to the flasks. The mixtures were then agitated at 120 rpm for contact times ranging from 5 to 90 min to attain equilibrium. A contact time of 90 min was determined to be sufficient for achieving equilibrium based on preliminary experiments. The second experiment focused on studying the pH of the adsorbate solution. The pH values of Cd(II) or Pb(II) solutions were adjusted to 5.0, 5.5, 6.0, 6.5, and 7.0 using 1 M HNO_3 (Merck) or 1 M NaOH (Merck) solutions. Subsequently, 50 mL of Cd(II) (50 mg/L) or Pb(II) solution (90 mg/L) and

0.10 g of moss biomass were added to 250-mL Erlenmeyer flasks and agitated for 60 min at 120 rpm. The third experiment examined the effect of adsorbent dosage. Moss biomass at different doses, namely 0.10 (0.2 % w/v), 0.25 (0.5 % w/v), and 0.50 (1.0 % w/v) g, respectively, were added into the flasks containing 50 mL of either Cd(II) or Pb(II) solutions with varying concentrations (5, 10, 15, 30, 50, 70, and 90 mg/L), with pH of 5.5 and a contact time of 60 min at 120 rpm.

Once metal adsorption was completed in each experiment, 15 mL of each mixture was centrifuged at 4000 rpm for 3 min, and the supernatant was filtered using pre-washed Whatman No. 42 filter paper with 2 % nitric acid for 1 min. The filtrate was then analysed for residual Pb or Cd content using a flame atomic absorption spectrometer (FAAS). The adsorption experiments were conducted in triplicate. As a control, 50 mL of a solution containing either Cd(II) or Pb(II) was placed in a 250-mL Erlenmeyer flask without the addition of biomass. The removal efficiency (E, %) serves as a measure of the effectiveness of the adsorbent material in eliminating heavy metal ions from the aqueous solution. It is calculated using the initial and final concentrations of heavy metals based on Equation (1), as described by Phaenark et al. [36].

$$E = \frac{(C_i - C_f)}{C_i} \times 100\% \quad (1)$$

Where C_i and C_f are the initial and remaining concentrations (mg/L) in the solution, respectively.

2.5. Equilibrium adsorption isotherms

We examined the adsorption of Cd(II) and Pb(II) onto moss biomass, using a dose of 0.1 g or 0.2 % w/v, while varying their concentrations (5, 10, 15, 30, 50, 70, and 90 mg/L for Cd(II) and Pb(II) solutions) to establish the isotherm. All other factors, including the optimal dose, contact time for each metal, temperature, and pH, remained constant. The equilibrium metal adsorption (q_e) was calculated using Equation (2), following Abdul Salim et al. [37].

$$q_e = \frac{(C_i - C_e) \times V}{W} \quad (2)$$

Where q_e (mg/g) is the total metal uptake at equilibrium, C_i (mg/L) is the initial concentration of metal ions, C_e (mg/L) is the equilibrium concentration of metal ions in solution, V (mL) is the solution volume, and W (mg) is the adsorbent weight.

In this study, we aimed to elucidate the adsorption mechanism by comparing the best fit of two-parameter linear isotherm models (Langmuir, Freundlich, and Elovich) and three-parameter linearized isotherm models (Sips and Redlich-Peterson) using experimental equilibrium data of Cd(II) and Pb(II) ions onto moss biomass particles. Our preliminary investigation of metal adsorption suggested that chemical sorption may occur via the functional groups of moss biomass, involving chemical bonding and ion exchange. Table 1 summarises the isotherms, their linear forms, and characteristic parameters.

2.6. Kinetic studies

Adsorption kinetics were evaluated through batch adsorption experiments, where initial metal concentrations of 50 mg/L for Cd(II) solution and 90 mg/L for Pb(II) solution were tested. The experiments involved various contact time intervals ranging from 5 min to 90 min, with the initial pH set at 5.5. To analyse the kinetics of the adsorption process, we apply the pseudo-first-order and pseudo-second-order models, as described by Febrianto et al. [40].

Equation (3) represents the pseudo-first-order model used in this study for the adsorption of metals onto biomass.

$$\ln(q_e - q_t) = \ln(q_e) - k_1 t_i \quad (3)$$

where q_e represents the amount of metal ions adsorbed at equilibrium per unit mass of adsorbent (mg/g), q_t denotes the same quantity at a particular adsorption time (mg/g), k_1 stands for the pseudo-first-order biosorption rate constant (min^{-1}), and t_i signifies the adsorption time (min).

Table 1
Two- and three-parameter isotherm models tested in the present study.

Isotherm model	Linear/Linearized form	Characteristic parameters	Reference
Two-parameter isotherm			
Langmuir	$\frac{1}{q_e} = \frac{1}{K_L q_{max} C_e} + \frac{1}{q_{max}}$	q_{max} = maximum adsorption capacity of adsorbent (mg/g), K_L = Langmuir constant (L/mg)	[37]
Freundlich	$\ln q_e = \ln K_F + \frac{1}{n} \ln C_e$	K_F = Freundlich constant (mg/g), n (dimensionless) = heterogeneity factor	[37]
Elovich	$\ln \frac{q_e}{C_e} = \ln K_E q_m - \frac{q_e}{q_m}$	q_m = maximum adsorbate uptake, K_E = Elovich equilibrium constant (L/mg)	[38]
Three-parameter isotherm			
Sips	$\beta_s \ln C_e = -\ln\left(\frac{K_S}{q_e}\right) + \ln(a_s)$	β_s = Sips isotherm exponent, K_s = Sips isotherm model constant (L/g), a_s = Sips isotherm model constant (L/g)	[38]
Redlich-Peterson	$\ln\left(K_R \frac{C_e}{q_e} - 1\right) = g \ln C_e + \ln a_R$	K_R = Redlich-Peterson adsorption isotherm constant, a_R = Redlich-Peterson constant; g = exponent that lie between 0 and 1	[39]

Equation (4) illustrates the pseudo-second-order kinetic model employed in this study.

$$\frac{t_i}{q_t} = \frac{1}{k_2 q_e^2} + \frac{t_i}{q_e} \tag{4}$$

where q_t is the mass of metal ions absorbed at adsorption time t (mg/g), q_e is the mass of metal ions adsorbed at equilibrium per unit mass of adsorbent (mg/g), k_2 is the pseudo-second-order biosorption rate constant (min^{-1}), and t_i is the adsorption time (min).

2.7. Statistical analyses

The study compared the variance in mean heavy metal adsorption efficiency among different experimental groups using one-way analysis of variance (ANOVA). If the means were found to be different, multiple comparisons were conducted to identify distinct pairs using Fisher's Least Significant Difference (LSD) method at a significance level of 0.05 using SPSS version 18.

2.8. Post-sorption characterisations of specific heavy metals

To identify specific functional groups present in the tested moss biomass, we conducted Fourier-transform infrared spectroscopy (FTIR) ranging from 4000–400 cm^{-1} with a resolution of 4 cm^{-1} and 32 scans, utilising attenuated total reflection with a diamond crystal parameter. This analysis was performed using a Nicolet iZ10 FTIR spectrometer (Thermo Scientific, USA). Additionally, energy dispersive X-ray (EDS) analysis was employed to examine the surface morphology and elemental composition of both pre-sorption and post-sorption moss biomass.

For the EDS analysis, the tested ground moss samples were mounted on carbon stubs using carbon conductive tape. These samples were then placed under a JEOL JSM-IT200 SEM equipped with an EDS system. Throughout the operation, the instrument's accelerating voltage was maintained at 20 kV, and varying magnifications were utilised for analysis.

3. Results and discussion

3.1. Biomass characterisation

The BET analysis revealed that the biomass from *B. consanguinea* (3.665 m^2/g) has a smaller surface area compared to the biomass from *H. involuta* (7.823 m^2/g), indicating the smaller adsorptive surface area of *B. consanguinea*. However, the total BJH pore volumes (0.014 cm^3/g for *B. consanguinea*; 0.015 cm^3/g for *H. involuta*) and the total micropore size distribution (1.749 nm for *B. consanguinea*; 1.871 nm for *H. involuta*) are quite similar between the two moss species.

The zeta potential of the biomass from *B. consanguinea* was recorded as -30 ± 0.1 mV, whereas that from *H. involuta* was -18.7 ± 1.8 mV. The higher net negative charge observed in *B. consanguinea* biomass suggests its enhanced capability to attract more highly positively charged heavy metal ions compared to *H. involuta* biomass. It is worth noting that the positive or negative values of zeta

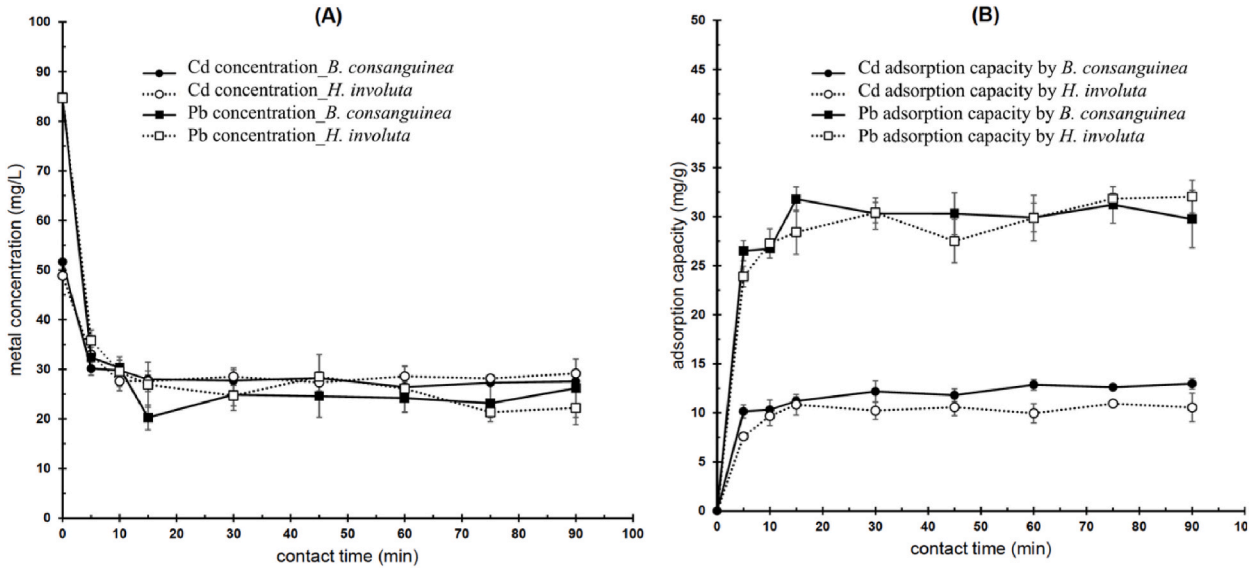

Fig. 2. The duration of contact impacts the adsorption of Cd(II) and Pb(II) ions by the biomass from mosses *B. consanguinea* and *H. involuta*, given optimal conditions, where the pH is 5.5 and the dose is 0.2 % w/v. (A) represents the metal concentrations (mg/L) remaining in solutions at various contact times, while (B) represents the adsorption capacity (mg/g) at different contact times.

potential are determined by the functional groups present on the adsorbent surface, as well as the pH value of the solution [41].

3.2. Effect of contact time

In Fig. 2, we observe a rapid initial adsorption rate, where approximately 32–62 % (Tables S1–S2) of the total Cd(II) and Pb(II) ions are removed within 5 min by biomass from *B. consanguinea* and *H. involuta* (Fig. 2A). Following this, the adsorption capacity gradually increases with contact time until it plateaus at 30 min (Fig. 2B). Therefore, we established 30 min as the equilibrium time, which proved sufficient for Cd(II) ion removal by this moss biomass biosorbent. Subsequent experiments maintained a contact time of 60 min to ensure adsorption equilibrium. The time curves depicted in Fig. 2 display smooth and continuous trends, indicating saturation and suggesting the potential for monolayer coverage of Cd(II) and Pb(II) ions on the adsorbent surface.

The amount of adsorbed Cd(II) and Pb(II) ions per unit mass of moss biosorbent (q_e), starting from an initial concentration of 50 mg/L for Cd(II) solution and 90 mg/L for Pb(II) solution after a 30-min equilibrium time, was 12.17 ± 1.08 mg/g for Cd(II) and 30.31 ± 1.59 mg/g for Pb(II) by biomass of *B. consanguinea*, and 10.23 ± 0.89 mg/g for Cd(II) and 30.40 ± 1.03 mg/g for Pb(II) by biomass of *H. involuta* (Table S1 and Table S2).

The initial rapid adsorption rate can be attributed to the abundance of free binding sites. During the initial stages of the adsorption process, the porous surface of moss biomass becomes nearly saturated with Cd(II) and Pb(II) ions. As adsorption progresses, Cd(II) and Pb(II) ions must travel deeper into the micro-pores, encountering increased resistance, which subsequently decreases the driving force and adsorption rate [42]. Furthermore, as adsorption continues, the desorption rate rises, impacting the adsorption-desorption equilibrium around the equilibrium point [42].

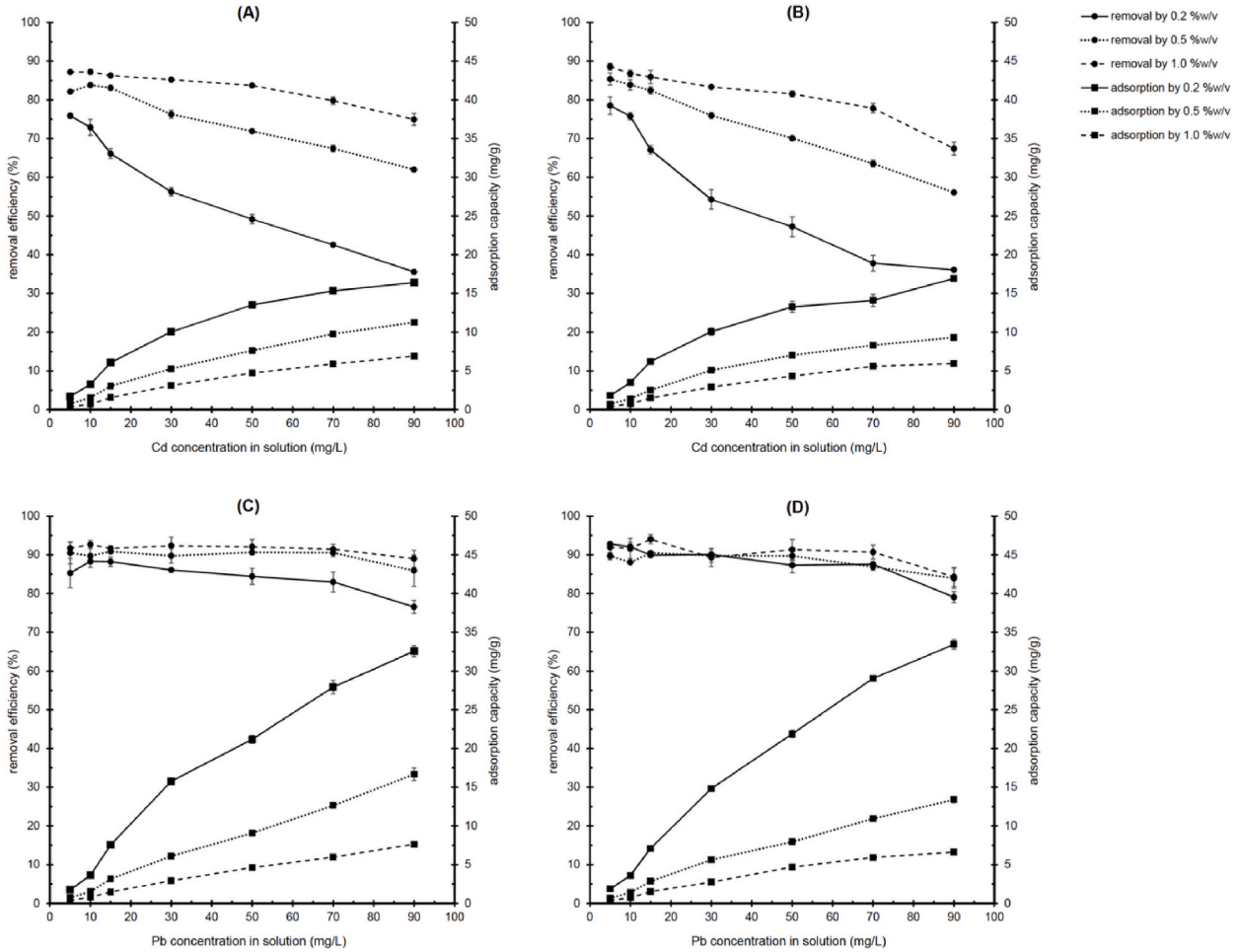

Fig. 3. The effect of initial concentrations of metal solutions and doses of moss biomass on the removal efficiency (%) and adsorption capacity (mg/g) of Cd(II) and Pb(II) ions by biomass from *B. consanguinea* and *H. involuta*. The investigation was conducted under optimal conditions of pH 5.5 and a contact time of 60 min. Designations A, B, C, and D represent the following combinations: A = Cd + *B. consanguinea*, B = Cd + *H. involuta*, C = Pb + *B. consanguinea*, and D = Pb + *H. involuta*, respectively.

3.3. Effect of initial concentrations of metal solution

Fig. 3 depicts the impact of varying initial concentrations of Cd(II) and Pb(II) solutions on the removal efficiency (%) and adsorption capacity (mg/g) of these metal ions by moss biomass. Regarding the effect of initial concentration on removal efficiency, for both Cd(II) and Pb(II), the removal efficiency of *B. consanguinea* biomass (Fig. 3A and C) and *H. involuta* biomass (Fig. 3B and D) generally decreases as the initial concentration of the metal ion in the solution increases across all doses of biomass. This observation can be attributed to the fact that the initial concentration of Cd(II) and Pb(II) solutions has a limited effect on metal removal capacity. Simultaneously, the moss biomass adsorbent possesses a limited number of active sites, which become saturated at a certain concentration. Consequently, there is an escalation in the number of Cd(II) and Pb(II) ions competing for the available functional groups on the surface of the adsorbent material. Since solutions with lower concentrations contain fewer free metal ions compared to those with higher concentrations, the percent removal decreases with increasing initial concentrations of metal solutions [43].

The decreasing trend in the removal efficiency of Cd(II) and Pb(II) by moss biomass corresponds to an increase in the adsorption capacity of the biomass adsorbent as the initial concentration increases (Fig. 3A–D) until the metal ions reach equilibrium saturation across all doses of biomass [44]. The heightened collision efficiency between the metal ions and these moss biomass biosorbents is likely due to the increasing initial concentration of Cd(II) and Pb(II) ions in the solution. However, the adsorption capacities of the metal ions remain nearly unchanged after reaching equilibrium saturation [45]. This lack of significant change may stem from the limited availability of active sites for adsorbing metal ions on the biosorbent surfaces, which impedes further adsorption [46].

Overall, both *B. consanguinea* and *H. involuta* biomass effectively removed Cd(II) and Pb(II) ions from contaminated water, although their efficiency depended on the initial concentration of metal solutions. The biomass from the two moss species exhibited higher effectiveness for removing Pb(II) (Fig. 3C and D) compared to Cd(II) (Fig. 3A and B). The optimal initial concentrations of Cd(II) and Pb (II) solutions for achieving maximum Cd (87 %) and Pb (93 %) removal efficiency by *B. consanguinea* biomass are 10 mg/L, with a dose of 1 % w/v biomass, a pH of 5.5, and a contact time of 60 min. In contrast, the optimal initial concentrations of Cd(II) and Pb(II) solutions for achieving maximum Cd (89 %) and Pb (94 %) removal efficiency by *H. involuta* biomass are 5 mg/L and 15 mg/L, respectively. This is achieved using a dose of 1 % w/v biomass, a pH of 5.5, and a contact time of 60 min (Tables S3 and S4).

3.4. Effect of doses of moss biosorbent

At a given initial concentration of metal ions, the dosage of the biosorbent determines the capacity of the adsorbent and is an important parameter. The adsorption capacity for Cd(II) and Pb(II) ions as a function of biomass dosage was explored in Fig. 3. The figure shows that increasing the dosage of *B. consanguinea* and *H. involuta* biomass from 0.2 % to 1.0 % w/v biomass results in a significant increase in removal efficiency, corresponding to a decrease in biosorption capacity. The probable reason for the increase in removal efficiency with an increase in biomass doses is that the higher number of possible binding sites and increased surface area of the biosorbent promote biosorption for Cd(II) and Pb(II) ions [45].

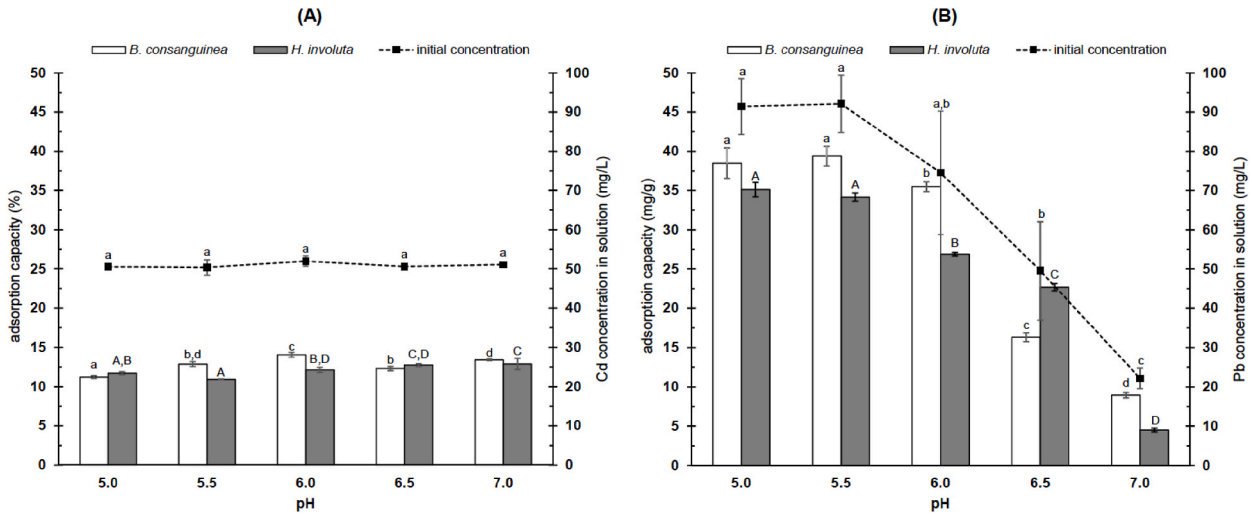

Fig. 4. The impact of solution pH on the adsorption capacity of Cd(II) ions (A) and Pb(II) ions (B) by *B. consanguinea* and *H. involuta* biomass was investigated under optimal conditions, including 0.1 g of biomass (0.2 % w/v) and a contact time of 60 min. The initial concentration for the Cd(II) solution is 50 mg/L, while for the Pb(II) solution, it is 90 mg/L. The significance of differences ($p < 0.05$) between the values denoted as a, b, c, d is determined by the LSD post hoc test within *B. consanguinea* biomass and the initial concentration of the metal solution, whereas the significance of differences ($p < 0.05$) between the values denoted as A, B, C, D is determined by the LSD post hoc test within *H. involuta* biomass.

3.5. Effect of solution pH

Fig. 4 demonstrates that the pH of the solution, ranging from 5.0 to 7.0, insignificantly affects the adsorption capacity of biomass from the two mosses for removing Cd(II) ions from aqueous solutions (Fig. 4A). However, the pH significantly influences the ability of biomass from the two mosses to remove Pb(II) ions from aqueous solutions. The optimum pH for the biosorption of Pb(II) by moss biomass occurs at a pH not greater than 6.0 (Fig. 4B). The decreasing trend in the adsorption capacity of Pb(II) ions corresponds with the decreasing trend of initial concentrations of Pb(II) solutions, suggesting the precipitation of Pb(II) ions in aqueous solutions as the pH increases (Fig. 4B). Consequently, assessing the adsorption capacity of moss biomass becomes challenging under such circumstances. It is possible that the relationship between Pb absorption and solution pH is closely connected not just to the surface functional groups on the biomass cell walls, but also to the species inside the cell and the speciation of the metal in solution [47].

Table 2
The equilibrium isotherm models, parameters, and their error analyses for the adsorption of Cd(II) and Pb(II) onto moss biomass of *B. consanguinea* and *H. involuta*.

Isotherm model[a]	*B. consanguinea*		*H. involuta*	
	Cd	Pb	Cd	Pb
Two - Parameter Isotherm				
Langmuir Isotherm				
q_{max} (mg/g)	17.0436	73.4455	15.5746	36.2828
K_L (L/mg)	0.1013	0.0546	0.1315	0.1854
Error analysis				
R^2	0.9980	0.9992	0.9971	0.9963
Root Mean Square Error	0.0081	0.0025	0.0090	0.0108
Mean Absolute Error	0.0076	0.0019	0.0076	0.0096
Mean Squared Error	0.0001	0.0000	0.0001	0.0001
Relative Absolute Error	0.0526	0.0260	0.0566	0.0640
Freundlich Isotherm				
$1/n$	0.5699	0.8166	0.5230	0.8115
K_F (mg/g)	1.8872	3.9851	2.1248	5.1785
Error analysis				
R^2	0.9813	0.9957	0.9821	0.9970
Root Mean Square Error	0.0476	0.0213	0.0447	0.0234
Mean Absolute Error	0.0425	0.0193	0.0421	0.0197
Mean Squared Error	0.0023	0.0005	0.0020	0.0005
Root Absolute Error	0.1387	0.0666	0.1444	0.0513
Elovich Isotherm				
q_m (mg/g)	9.0370	51.3606	7.6218	46.1501
K_E (L/mg)	0.2138	0.0814	0.3060	0.1318
Error analysis				
R^2	0.9871	0.9824	0.9824	0.8374
Root Mean Square Error	0.0691	0.0230	0.0932	0.0944
Mean Absolute Error	0.0483	0.0193	0.0730	0.0843
Mean Squared Error	0.0048	0.0005	0.0087	0.0089
Relative Absolute Error	0.0894	0.1258	0.1146	0.4316
Three – Parameter Isotherm				
Sips Isotherm				
K_s (L/g)	1.7235	3.9069	1.9660	–
a_s	0.0799	0.0238	0.0472	–
β_s	0.8904	0.9176	0.6898	–
Error analysis				
R^2	0.9998	0.9977	0.9926	–
Relative Mean Square Error	0.0026	0.0042	0.0144	–
Mean Absolute Error	0.0022	0.0033	0.0111	–
Mean Squared Error	0.0000	0.0000	0.0002	–
Relative Absolute Error	0.0153	0.0440	0.0832	–
Redlich-Peterson Isotherm				
K_R (L/g)	1.6566	4.5238	2.7874	–
a_R (L/mg)	0.1165	0.1554	0.4686	–
g	0.9185	0.6971	0.7268	–
Error analysis				
R^2	0.9981	0.9856	0.9932	–
Relative Mean Square Error	0.0450	0.0068	0.0940	–
Mean Absolute Error	0.0420	0.0058	0.0659	–
Mean Squared Error	0.0020	0.0000	0.0088	–
Relative Absolute Error	0.0474	0.1164	0.0653	–

[a] The isotherm model parameters and error values were estimated using the PUPAIM package in R software.

3.6. Adsorption isotherms

Many adsorption isotherms have been applied for modelling experimental data on equilibrium adsorption. In this study, various adsorption isotherm models of solid-liquid phases are selected (Table 1) and discussed because they are commonly used in the literature.

Table 2 presents the results of linearized fitting for the selected adsorption isotherm models. The coefficient of determination (R^2), exceeding 0.98, and other error functions, including root mean square error (RMSE), mean absolute error (MAE), mean squared error (MSE), and relative absolute error (RAE), indicate consistently small values across the models. These findings suggest that the experimental data for the adsorption process aligned well with nearly all selected models [48], except for the Elovich model for Pb(II) adsorption onto biomass from *H. involuta*, which demonstrated a slightly lower R^2 value than 0.98. Furthermore, the Sips and Redlich-Peterson models for Pb(II) adsorption onto biomass from *H. involuta* did not adequately fit the data. The fitting of each isotherm to our experimental data is discussed in more detail below.

The Langmuir isotherm, an empirical model utilised to describe adsorption phenomena, posits that adsorption occurs at identical sites with a monolayer thickness and uniform adsorption force. Initially developed for gas-solid phase adsorption, this model has been extended to liquid systems. At equilibrium, adsorption and desorption rates are equal and regulated by the equilibrium constant [34]. In this study, the Langmuir model aptly describes the adsorption of Cd(II) and Pb(II) onto biomass from both *B. consanguinea* and *H. involuta*, with R^2 values exceeding 0.99 (Table 2). The adsorption capacities, represented by q_{max}, are higher for Pb(II) (73.4455 and 36.2828 mg/g) compared to Cd(II) (17.0436 and 15.5746 mg/g) onto a monolayer homogeneous surface of moss biomass from *B. consanguinea* and *H. involuta*, respectively.

The Freundlich isotherm, an empirical model, is commonly utilised to describe adsorption phenomena, particularly organic pollutants and heavy metals on various adsorbents. Unlike the Langmuir model, Freundlich considers a heterogeneous surface with multiple types of adsorption sites and can account for both monolayer adsorption when chemisorption prevails and multilayer adsorption when physisorption dominates [34]. In this study, the Freundlich model demonstrates a better fit for the adsorption of Pb (II) ($R^2 > 0.99$) compared to Cd(II) adsorption ($R^2 > 0.98$). The calculated K_F values for Pb(II) (3.9851 and 5.1785 mg/g) are higher than those for Cd(II) (1.8872 and 2.1248 mg/g) onto biomass from *B. consanguinea* and *H. involuta*, respectively, indicating higher adsorption capacities (Table 2).

The Elovich model is rooted in the kinetic principle, assuming that adsorption sites increase exponentially with adsorption, thereby suggesting multilayer adsorption [49]. Despite the model's suitability for Cd(II) and Pb(II) adsorption onto biomass from *B. consanguinea* ($R^2 > 0.98$) and for Cd(II) adsorption onto biomass from *H. involuta* ($R^2 > 0.98$) (Table 2), the calculated adsorption capacities, denoted by q_m, were relatively low compared to q_{max} values obtained from the Langmuir model. This discrepancy may stem from the Elovich model's description of multilayer adsorption, suggesting migration from one layer to another [50].

The Sips isotherm, a hybrid model that combines elements from both the Langmuir and Freundlich isotherm models [51], offers significant advantages in predicting monolayer adsorption in both homogeneous and heterogeneous systems. By addressing the limitations associated with increased concentrations of the adsorbate, which are characteristic of the Freundlich model [52], the Sips model provides enhanced accuracy in describing adsorption isotherms. This incorporation of features from both the Langmuir and Freundlich models makes it particularly suitable for metal adsorbents, including biosorbents. In this study, our experimental data showed good agreement with the Sips model, with R^2 values exceeding 0.99 for Cd(II) adsorption onto biomass from both *B. consanguinea* and *H. involuta*, as well as for Pb(II) adsorption onto biomass from *B. consanguinea*. However, the Sips model did not fit well for Pb(II) adsorption onto biomass from *H. involuta* (Table 2).

The Redlich-Peterson model, another empirical hybrid of the Langmuir and Freundlich models, is often used in both homogeneous and heterogeneous adsorption processes [52]. Like the Sips model, our results indicate that the Redlich-Peterson isotherm best describes the equilibrium data, confirming adsorption of Cd(II) onto biomass from both *B. consanguinea* and *H. involuta*, as well as Pb(II) adsorption onto *B. consanguinea*.

In this study, we investigated two kinetic models, namely the pseudo-first-order and pseudo-second-order, to describe the adsorption of Cd(II) and Pb(II) ions by moss biomass. We calculated correlation coefficients (R^2), experimental and computed values of metal uptake capacity, and rate constants for both models at various initial concentrations of Pb(II) and Cd(II) ions. The findings are summarised in Table 3. Our results show that the pseudo-second-order kinetic model best describes the adsorption of Cd(II) and Pb(II) ions by biomass from *B. consanguinea* (Cd: $R^2 = 1.000$, Pb: $R^2 = 0.999$) and *H. involuta* (Cd: $R^2 = 0.999$; Pb: $R^2 = 0.998$) (Table 3). This

Table 3
Pseudo-first-order and pseudo-second-order kinetic constants for Cd(II) and Pb(II) ion adsorption by biomass prepared *B. consanguinea* and *H. involuta*.

Biomass	Metal ion	Metal adsorption	Pseudo-first-order kinetic model			Pseudo-second-order kinetic model		
		$q_{e,exp}$ (mg/g)	$q_{e,cal}$ (mg/g)	K_1 x 10^2 (1/min)	R^2	$q_{e,cal}$ (mg/g)	K_2 (g/(mg • min))	R^2
B. consanguinea	Cd	13.538	3.343	1.920	0.935	13.210	0.032	1.000
	Pb	32.555	6.803	2.010	0.928	30.395	0.089	0.999
H. involuta	Cd	13.273	5.247	0.910	0.728	10.858	0.075	0.999
	Pb	33.427	8.417	1.970	0.912	32.362	0.014	0.998

*Condition for Cd(II) kinetic study: 0.2 % w/v biomass, 50 mg/L Cd, pH = 5.5.
**Condition for Pb(II) kinetic study: 0.2 % w/v biomass, 90 mg/L Pb, pH = 5.5.

suggests that the biomass from both moss species exhibits a tendency for chemisorption [37,53].

The short-term uptake of cations by moss is generally understood to be an abiotic process, as highlighted in prior research [54]. This process is regulated by several mechanisms. Firstly, cations can undergo surface complexation by binding to exposed functional groups, including carboxyl, sulfhydryl, and amine, among others, present in the moss biomass. Secondly, ion exchange plays a significant role in the process. Additionally, the coordination and chelation of metals contribute to the uptake mechanism. Furthermore, adsorption onto the moss surface is another significant mechanism facilitating cation uptake. Lastly, the precipitation of solid phases on the cell walls of the moss represents yet another mechanism involved in this process [55,56]. Table 4 provides a comparative analysis of the adsorption capacities of various bryophyte species as biosorbents for Cd(II) and Pb(II) removal. The data suggest that moss biomass holds significant promise as a highly effective adsorbent for eliminating Cd(II) and Pb(II) ions from polluted water sources.

3.7. Functional group characteristics of biomass

The functional group characteristics of the original and loaded biomass from mosses *B. consanguinea* and *H. involuta* were investigated using FTIR studies (Figs. 5 and 6). The peaks in the FTIR spectra of the original biomass of both moss species exhibit similar patterns (Figs. 5A and 6A), showing peaks at 3300 cm^{-1} indicative of –OH groups or at 3267 cm^{-1} indicative of –NH groups from phenols, alkaloids, or amines [65]. The stretching band at 2900–2800 cm^{-1} is related to the alkene –C–H bond [66]. The peak at 1595 cm^{-1} corresponds to nitro compounds (N–O) [65], and the peaks at 1300–600 cm^{-1} are attributed to low-molecular-weight carbohydrates, polyols, and monosaccharides [67], respectively.

In Fig. 5B and C, it is evident that the *B. consanguinea* biomass, upon contact with Cd(II) and Pb(II) respectively, exhibits a noticeable shift in the infrared spectrum peak to the right. This shift is attributed to certain functional groups, such as –OH or –NH functional groups found in phenols, alkaloids, or amines (3280 cm^{-1}), and low-molecular-weight carbohydrates, polyols, and monosaccharides (1034, 521, 455, and 436 cm^{-1}) following Cd(II) adsorption. Similarly, following Pb(II) adsorption, the corresponding functional groups observed are –OH or –NH functional groups of phenols, alkaloids, or amines (3282 cm^{-1}), alkene –C–H bonds (2885 cm^{-1}), nitro compounds or N–O groups (1587 cm^{-1}), and low-molecular-weight carbohydrates, polyols, and monosaccharides (1011, 542, 517, and 461 cm^{-1}).

In Fig. 6B and C, it is observed that the *H. involuta* biomass, upon contact with Cd(II) and Pb(II) respectively, exhibits a shift in the infrared spectrum peak to the right to a certain extent. The corresponding functional groups that shifted include –OH or –NH functional groups found in phenols, alkaloids, or amines (3257 cm^{-1} for Cd(II) adsorption and 3253 cm^{-1} for Pb(II) adsorption), alkene –C–H bonds (2904 cm^{-1} for Cd(II) adsorption and 2908 cm^{-1} for Pb(II) adsorption), nitro compounds or N–O groups (1593 cm^{-1} for Cd(II) adsorption and 1589 cm^{-1} for Pb(II) adsorption), and low-molecular-weight carbohydrates, polyols, and monosaccharides (1009, 511, and 438 cm^{-1} for Cd(II) adsorption and 1009, 478, and 438 cm^{-1} for Pb(II) adsorption).

The observed shift in bands signifies the preferential involvement of specific functional groups in bonding with metals. Indeed, various authors have highlighted the significant role of these functional groups in the uptake of Cd(II) and Pb(II) by different types of moss biomass. For example, Sari et al. [68] employed FTIR spectroscopy to study the biosorption of palladium(II) from aqueous solutions using aquatic moss (*Racomitrium lanuginosum*) biomass. They noted an ion-exchange process between Pd(II) ions and the hydrogen atoms of –OH, $–NH_2$, and –COOH functional groups present in the moss biomass. Similar mechanisms were observed in the biosorption of Cd(II) and Zn(II) ions using another aquatic moss, *Fontinalis antipyretica* [57], as well as in other terrestrial mosses such

Table 4
Comparison of adsorption capacities of Cd(II) and Pb(II) ions with bryophyte adsorbents determined by the Langmuir model in this study and those reported in the selected literature.

Adsorbent	q_{max} (mg/g)		Contact time (min)	T (°C)	pH	Reference
	Cd(II)	Pb(II)				
Ground biomass of *Fontinalis antipyretica*	28.000	–	60	20	5	[57]
Ground peat moss	33.900	91.74	120	–	–	[58]
Dried peat moss	–	117.580	240	5, 25, 55	6	[59]
Fresh *Hypnum* sp.	0.036	0.313	5	20	6–7	[22]
Fresh peat moss	0.082	0.230	5	20	6–7	[22]
Fresh *Pseudoscleropodium purum*	0.030	0.182	5	20	6–7	[22]
Fresh *Brachytecium rutabulum*	0.051	0.530	5	20	6–7	[22]
Ground biomass *Fontinalis antipyretica*	4.800	4.800	1440	20	5.0–5.2	[60]
Peat moss biochar (pyrolysis over a temperature range of 800 °C for 90 min)	39.800	81.300	–	–	–	[61]
Ground biomass *Vesicularia dubyana*	31.475	–	120	–	4–8	[62]
Pristine *Barbula lambarenensis* (RBL)	42.500	75.300	5–720	24–50	3–7	[63]
B. lambarenensis treated with sodium tripolyphosphate (TPP)	53.800	133.300	5–720	24–50	3–7	[63]
B. lambarenensis treated with ethylene glycol (EGP)	54.200	85.000	5–720	24–50	3–7	[63]
Dried biomass of peat moss (*Sphagnum palustre*)	–	0.042–0.104	480	20	5.5	[64]
Dried biomass of peat moss (*Sphagnum palustre*)	–	0.173–0.552	480	20	6.5	[64]
Ground biomass of moss *B. consanguinea*	17.044	73.446	60	25	5.5	This study
Ground biomass of moss *H. involuta*	15.575	36.283	60	25	5.5	This study

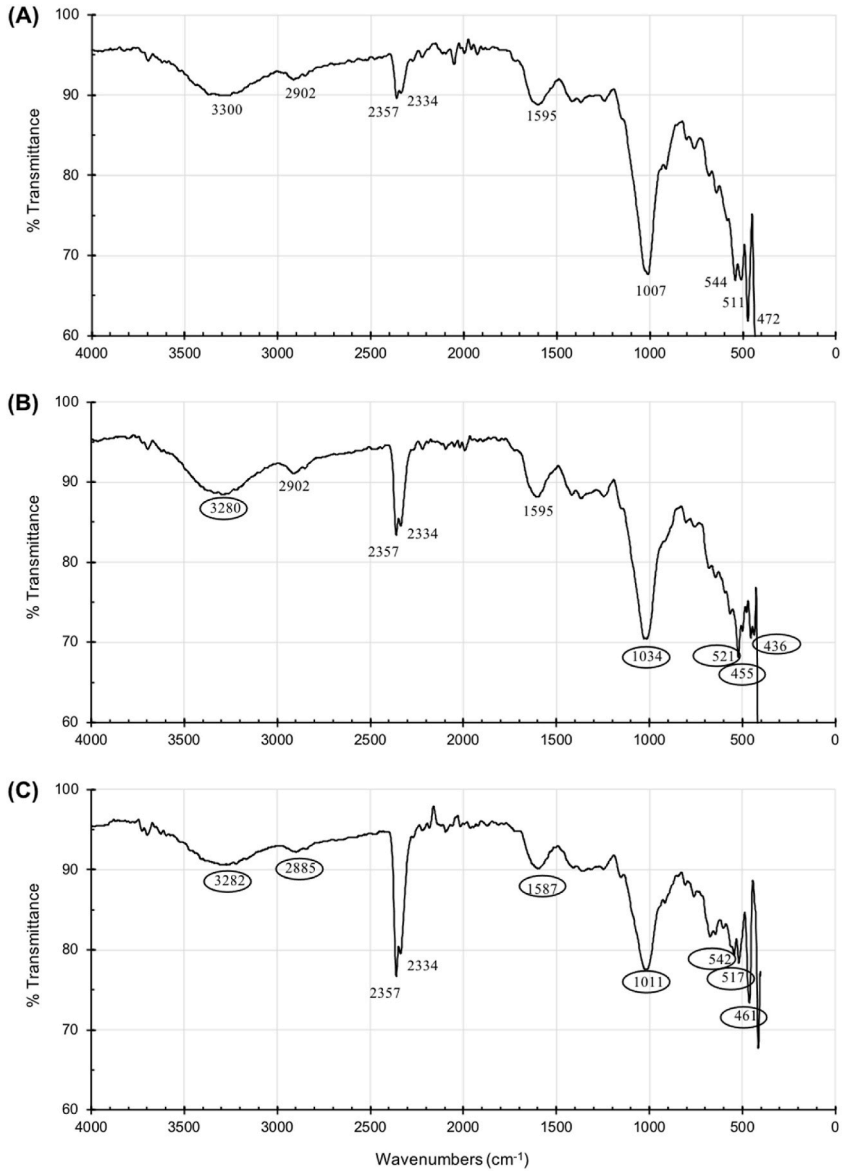

Fig. 5. FTIR spectrum of biomass of *B. consanguinea* prior to metal adsorption (A), after Cd adsorption (B), and after Pb adsorption (C).

as *Pleurozium schreberi* [69], *Hyloconium splendens* [70], and *Drespanocladus revolvens* [71].

3.8. EDS analysis

Figs. 7 and 8 display SEM scans of various moss biomass samples taken before and after metal adsorption at different treatment times. It is apparent that the surfaces of the gametophore lamina biomass exhibit high non-uniformity. Comparing images of the native adsorbent (Fig. 7A and 8A) with those after metal adsorption (Figs. 7B–C and 8B–C) reveals no discernible morphological alterations on the biomass surface following the adsorption of Cd(II) and Pb(II) ions. Elemental mapping clearly illustrates the uniform distribution of Cd(II) and Pb(II) onto the biomass surface (Figs. 7B–C and 8B–C). Moreover, EDX spectra obtained in spot profile mode confirm the presence of Cd(II) (Figs. 7B and 8B) and Pb(II) (Figs. 7C and 8C), indicating the bonding of metal cations to the biomass surface through interactions with negative charges of functional groups.

Observations on the gametophore lamina biomass of randomly selected spots post-adsorption indicate a decrease in the peak of Ca (II) in the EDX spectra of *B. consanguinea* biomass following Cd(II) and Pb(II) adsorption (Fig. 7B and C) compared to the native biomass (Fig. 7A). Similarly, a decrease in the peak of Ca(II) is observed in the EDX spectra of *H. involuta* biomass following Cd(II) and Pb(II) adsorption (Fig. 8B and C) compared to the native biosorbent (Fig. 8A). This suggests that Cd(II) and Pb(II) ions have displaced Ca(II) ions from the biomass surface, indicating an ion exchange mechanism involved in Cd(II) and Pb(II) biosorption. However, due to

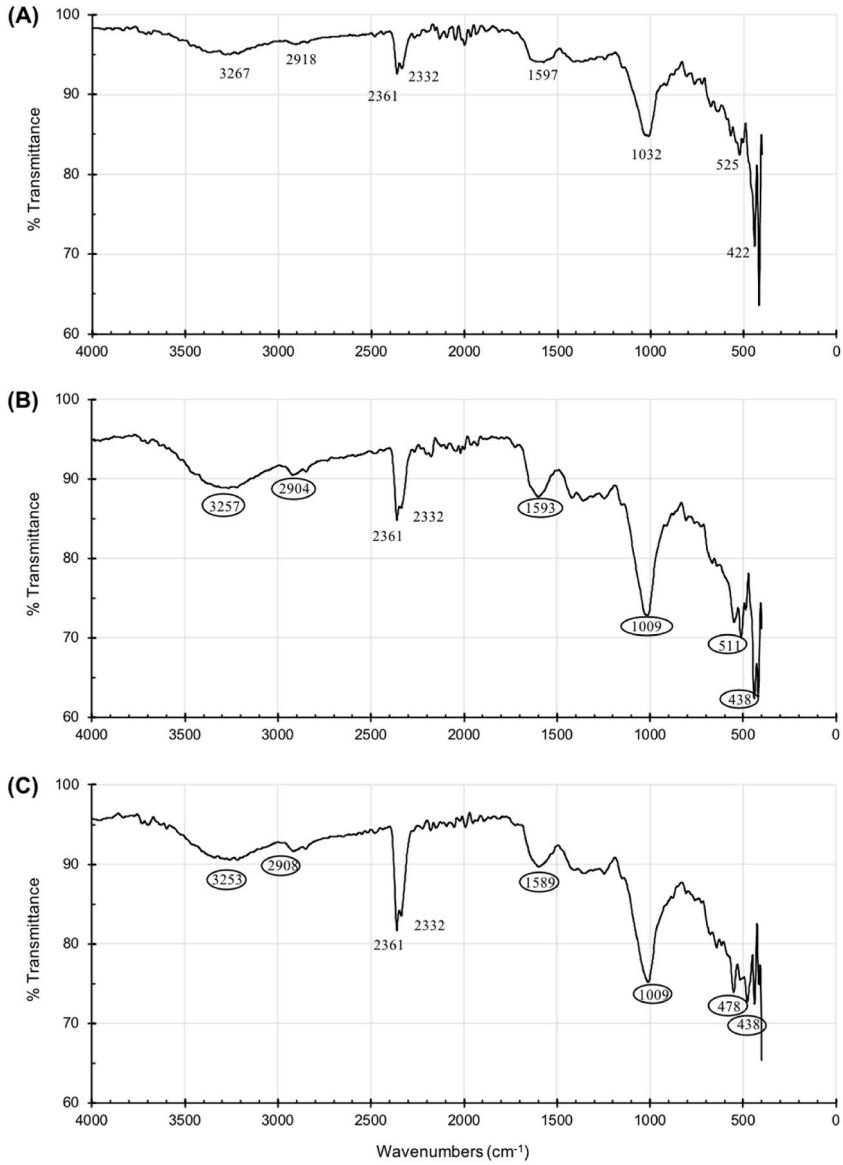

Fig. 6. FTIR spectrum of biomass of *H. involuta* prior to metal adsorption (A), after Cd adsorption (B), and after Pb adsorption (C).

the complexity of biomaterials, it is plausible that multiple mechanisms operate simultaneously, to varying degrees, contingent upon the biosorbent and solution chemistry [72]. Similar conclusions have been proposed in the literature by Sheng et al. [73], Iqbal et al. [74], and Marešová et al. [72].

4. Conclusions

The study investigated the kinetics and mechanisms of Cd(II) and Pb(II) ion removal using biomass from the mosses *Barbula consanguinea* and *Hyophila involuta*. The findings revealed rapid initial adsorption rates, with approximately 32–62 % of Cd(II) and Pb (II) ions removed within 5 min, followed by a gradual increase until equilibrium at 30 min, establishing it as the equilibrium time. Adsorption was pH-independent for Cd(II) but pH-dependent for Pb(II), with maximum removal occurring at pH 5.0–5.5. Higher q_{max} and K_F values for Pb(II) than for Cd(II) suggested a greater affinity for Pb(II).

Adsorption isotherm analysis indicates excellent alignment between the experimental data and most selected models (i.e., the Langmuir, Freundlich, Elovich, Sips, and Redlich-Peterson models) with ($R^2 > 0.98$), except for Pb(II) adsorption onto *H. involuta* biomass, where deviations were observed with the Elovich, Sips, and Redlich-Peterson models. The pseudo-second-order kinetic model best described the process, indicating chemisorption. FTIR spectra indicated major binding sites, including phenols, alkaloids, amines, alkenes, nitro compounds, and low-molecular-weight carbohydrates. According to the Langmuir model, adsorption was selective, with

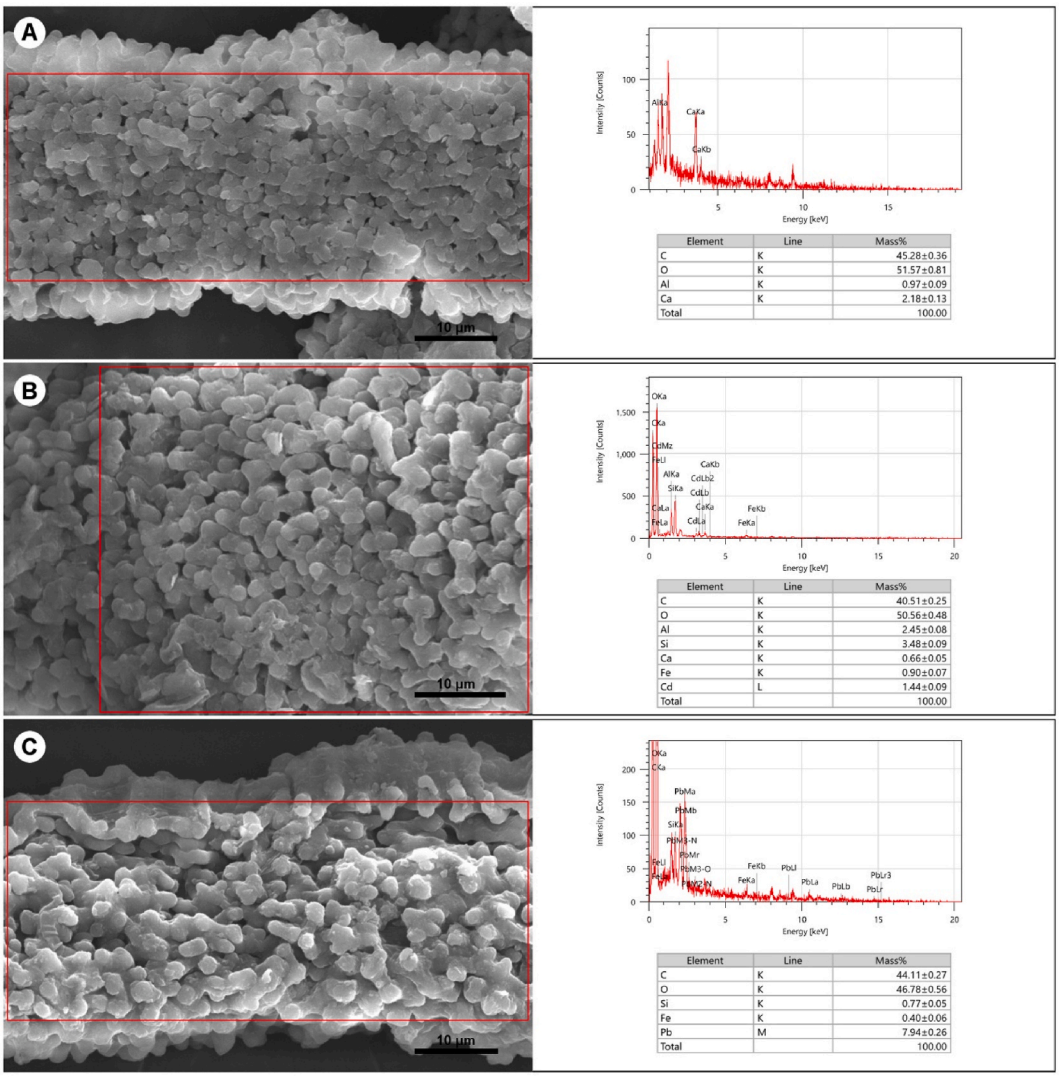

Fig. 7. Energy dispersive X-ray (EDX) analysis of the biomass of *B. consanguinea*: (A) before metal adsorption, (B) after the adsorption of Cd(II), and (C) after the adsorption of Pb(II).

Pb(II) > Cd(II), and *B. consanguinea* showed a higher adsorption capacity than *H. involuta* (Table 2).

The superior adsorption capacity of biomass from *B. consanguinea* is confirmed by its higher negative zeta potential compared to that of *H. involuta*. EDS analysis further confirmed the bonding of Cd(II) and Pb(II) ions to the biomass surface. This study highlights the potential of moss biomass as an effective biosorbent for the removal of Cd(II) and Pb(II) in water treatment, with significant implications for circular economy strategies focused on sustainable waste management and resource recovery.

Research limitations and future directions

While the study provides valuable insights into the removal of Cd(II) and Pb(II) ions using moss biomass, several limitations should be noted. Firstly, the research focuses solely on batch adsorption techniques, which may not fully capture the dynamics of adsorption processes in continuous flow systems. Secondly, the investigation primarily considers the adsorption efficiency in terms of contact time, initial metal ion concentration, adsorbent dose, and pH, potentially overlooking other influential factors such as temperature variations and the presence of competing ions in real-world water matrices. Additionally, the study employs biomass from only two moss species, limiting the generalizability of the findings to other moss species with potentially different adsorption capacities and mechanisms. Lastly, while the study identifies major binding sites using FTIR spectra and confirms metal ion bonding with biomass through EDS analysis, the specific mechanisms underlying adsorption remain incompletely elucidated, warranting further investigation.

Exploring the feasibility of regenerating biomass from mosses after its initial use holds significant promise for sustainable water

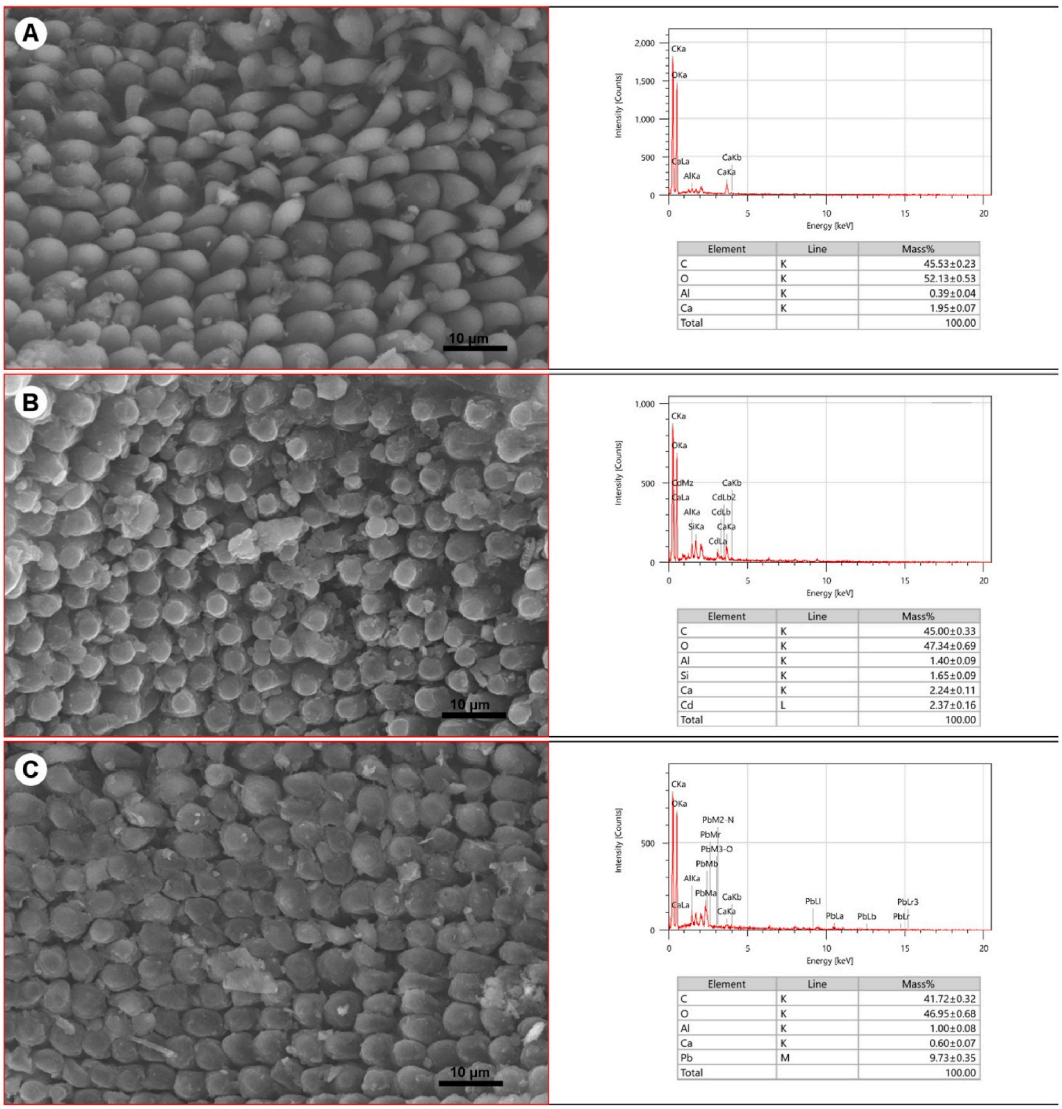

Fig. 8. Energy dispersive X-ray (EDX) analysis of the biomass of *H. involuta*: (A) before metal adsorption, (B) after the adsorption of Cd(II), and (C) after the adsorption of Pb(II).

treatment practices. By rejuvenating the moss biomass, we can potentially extend its lifespan and maximise its efficiency in adsorbing contaminants from water sources. In our next research endeavour, we aim to investigate several techniques for regenerating moss biomass. These techniques may include thermal treatment, chemical regeneration using desorbing agents, and physical methods such as washing or mechanical agitation. Each approach presents unique advantages and challenges, and our study will evaluate their effectiveness, cost-efficiency, and environmental impact to determine the most suitable regeneration method. According to Kettum et al. [27], the reusability of the functionalised carbon foams via repeated adsorption/desorption cycles is feasible. The spent adsorbents can be recovered by acid washing using 0.1 M HCl as the desorbing solution and 0.1 M NaOH as the regeneration solution. The regenerated carbon foams are then washed with distilled water to a neutral pH and reused in a new adsorption/desorption cycle. Ultimately, by establishing viable regeneration techniques, we can contribute to the development of sustainable water treatment strategies while minimising the environmental footprint associated with the disposal of spent moss biomass.

Funding

This research received no external funding.

Data availability

The data supporting the findings of this study can be obtained by reaching out to the corresponding author upon request.

CRediT authorship contribution statement

Chetsada Phaenark: Writing – review & editing, Writing – original draft, Visualization, Validation, Supervision, Software, Resources, Methodology, Investigation, Formal analysis, Data curation, Conceptualization. **Sarunya Nasuansujit:** Resources, Methodology, Investigation, Formal analysis, Data curation. **Natdanai Somprasong:** Software, Resources, Methodology, Investigation, Formal analysis, Data curation. **Weerachon Sawangproh:** Writing – review & editing, Writing – original draft, Visualization, Validation, Supervision, Software, Methodology, Investigation, Formal analysis, Data curation, Conceptualization.

Declaration of competing interest

The authors declare that they have no known competing financial interests or personal relationships that could have appeared to influence the work reported in this paper.

Acknowledgments

The authors would like to express their gratitude to Mahidol University (Kanchanaburi Campus) for providing the essential infrastructure and laboratory facilities. Special thanks are extended to Ms. Tiyanun Jurkvon from Mahidol University-Frontier Research Facility (MU-FRF) for her assistance in conducting the heavy metal analysis.

Appendix A. Supplementary data

Supplementary data to this article can be found online at https://doi.org/10.1016/j.heliyon.2024.e33097.

References

[1] S. Mishra, R.N. Bharagava, N. More, A. Yadav, S. Zainith, S. Mani, P. Chowdhary, Heavy metal contamination: an alarming threat to environment and human health, in: R.C. Sobti, N.K. Arora, R. Kothari (Eds.), Environmental Biotechnology: for Sustainable Future, Springer, Singapore, 2019, pp. 103–125, https://doi.org/10.1007/978-981-10-7284-0_5.

[2] M.I. Tudor, M. Tudor, C. David, L. Teodorof, D. Tudor, O. Ibram, Heavy metals concentrations in aquatic environment and living organisms in the danube delta, Romania, in: L. Simeonov, E. Chirila (Eds.), Chemicals as Intentional and Accidental Global Environmental Threats, Springer, Nordrecht, the Netherlands, 2006, pp. 435–442.

[3] P. Parkpian, S.T. Leong, P. Laortanakul, N. Thunthaisong, Regional monitoring of lead and cadmium contamination in a tropical grazing land site, Thailand, Environ. Monit. Assess. 85 (2003) 157–173.

[4] W. Nakbanpote, M.N. Prasad, B. Mongkhonsin, N. Panitlertumpai, R. Munjit, L. Rattanapolsan, Strategies for rehabilitation of mine waste/leachate in Thailand, in: M.N.V. Prasad, P.J.d.C. Favas, S.K. Maiti (Eds.), Bio-Geotechnologies for Mine Site Rehabilitation, Elsevier Inc., Amsterdam, Netherlands, 2018, pp. 617–643.

[5] C. Phaenark, A. Niamsuthi, P. Paejaroen, S. Chunchob, N. Cronberg, W. Sawangproh, Comparative toxicity of heavy metals Cd, Zn, and Pb to three acrocarpous moss species using chlorophyll contents, Trends Sci 20 (2023) 4287, https://doi.org/10.48048/tis.2023.4287.

[6] Z. Rahman, V.P. Singh, The relative impact of toxic heavy metals (THMs)(arsenic (As), cadmium (Cd), chromium (Cr)(VI), mercury (Hg), and lead (Pb) on the total environment: an overview, Environ. Monit. Assess. 191 (2019) 1–21, https://doi.org/10.1007/s10661-019-7528-7.

[7] G.A. Engwa, P.U. Ferdinand, F.N. Nwalo, M.N. Unachukwu, Mechanism and health effects of heavy metal toxicity in humans, in: O. Karcioglu, B. Arslan (Eds.), Poisoning in the Modern World, 10, IntechOpen, Croatia, 2019, pp. 77–99, https://doi.org/10.5772/intechopen.82511.

[8] S. Gheorghe, C. Stoica, G.G. Vasile, M. Nita-Lazar, E. Stanescu, I.E. Lucaciu, Metals toxic effects in aquatic ecosystems: modulators of water quality, in: H. Tutu (Ed.), Water Quality, IntechOpen, Croatia, 2017, pp. 59–89, https://doi.org/10.5772/65744.

[9] M. Kumar, A. Seth, A.K. Singh, M.S. Rajput, M. Sikandar, Remediation strategies for heavy metals contaminated ecosystem: a review, Environ. Sustain. Indic. 12 (2021) 100155, https://doi.org/10.1016/j.indic.2021.100155.

[10] C. Phaenark, T. Jantrasakul, P. Paejaroen, S. Chunchob, W. Sawangproh, Sugarcane bagasse and corn stalk biomass as a potential sorbent for the removal of Pb (II) and Cd(II) from aqueous solutions, Trends Sci 20 (2022) 6221, https://doi.org/10.48048/tis.2023.6221.

[11] R. Apiratikul, P. Pavasant, Batch and column studies of biosorption of heavy metals by *Caulerpa lentillifera*, Bioresour. Technol. 99 (2008) 2766–2777, https://doi.org/10.1016/j.biortech.2007.06.036.

[12] R. Gourdon, S. Bhende, E. Rus, S.S. Sofer, Comparison of cadmium biosorption by Gram-positive and Gram-negative bacteria from activated sludge, Biotechnol. Lett. 12 (1990) 839–842, https://doi.org/10.1007/BF01022606.

[13] A.R. Betts, N. Chen, J.G. Hamilton, D. Peak, Rates and mechanisms of Zn^{2+} adsorption on a meat and bonemeal biochar, Environ. Sci. Technol. 47 (2013) 14350–14357, https://doi.org/10.1021/es4032198.

[14] K. Yan, Y. Liu, Y. Lu, J. Chai, L. Sun, Catalytic application of layered double hydroxide-derived catalysts for the conversion of biomass-derived molecules, Catal. Sci. Technol. 7 (2017) 1622–1645, https://doi.org/10.1039/c7cy00274b.

[15] A. Wang, Z. Zheng, R. Li, D. Hu, Y. Lu, H. Luo, K. Yan, Biomass-derived porous carbon highly efficient for removal of Pb(II) and Cd(II), Green Energy Environ. 4 (2019) 414–423, https://doi.org/10.1016/j.gee.2019.05.002.

[16] S. Nickel, W. Schröder, Integrative evaluation of data derived from biomonitoring and models indicating atmospheric deposition of heavy metals, Environ. Sci. Pollut. Res. 24 (2017) 11919–11939, https://doi.org/10.1007/s11356-015-6006-1.

[17] C. Phaenark, P. Seechanhoi, W. Sawangproh, Metal toxicity in *Bryum coronatum* Schwaegrichen: impact on chlorophyll content, lamina cell structure, and metal accumulation. Int. J. Phytoremediation. 1-12. https://doi.org/10.1080/15226514.2024.2317878.

[18] A. Kłos, Z. Ziembik, M. Rajfur, A. Dołhańczuk-Śródka, Z. Bochenek, J.W. Bjerke, .P. Świsłowski, Using moss and lichens in biomonitoring of heavy-metal contamination of forest areas in southern and north-eastern Poland, Sci. Total Environ. 627 (2018) 438–449.

[19] J. Barukial, P. Hazarika, Bryophytes as an accumulator of toxic elements from the environment: recent advances, in: H.N. Murthy (Ed.), Bioactive Compounds in Bryophytes and Pteridophytes, Reference Series in Phytochemistry, Springer, Cham, Switzerland, 2023, pp. 165–182.

[20] A. Dreyer, S. Nickel, W. Schroder, Persistent) Organic pollutants in Germany: results from a pilot study within the 2015 moss survey, Environ. Sci. Eur. 30 (1) (2018) 43, https://doi.org/10.1186/s12302-018-0172-y[.

[21] Q. Wu, X. Wang, Q. Zhou, Biomonitoring persistent organic pollutants in the atmosphere with mosses: performance and application, Environ. Int. 66 (2014) 28–37.

[22] A.G. Gonzalez, O.S. Pokrovsky, Metal adsorption on mosses: toward a universal adsorption model, J. Colloid Interface Sci. 415 (2014) 169–178, https://doi.org/10.1016/j.jcis.2013.10.028.

[23] Z. Varela, M.T. Boquete, J.A. Fernández, J. Martínez-Abaigar, E. Núñez-Olivera, J.R. Aboal, Mythbusters: unravelling the pollutant uptake processes in mosses for air quality biomonitoring, Ecol. Indicat. 148 (2023) 110095, https://doi.org/10.1016/j.ecolind.2023.110095.

[24] A.G. Gonzalez, O.S. Pokrovsky, A.K. Beike, R. Reski, A. Di Palma, P. Adamo, G. Simonetta, J.A. Fernandez, Metal and proton adsorption capacities of natural and cloned *Sphagnum* mosses, J. Colloid Interface Sci. 461 (2016) 326–334, https://doi.org/10.1016/j.jcis.2015.09.012.

[25] P. Papadia, F. Barozzi, D. Migoni, M. Rojas, F.P. Fanizzi, G.P. Di Sansebastiano, Aquatic mosses as adaptable bio-filters for heavy metal removal from contaminated water, Int. J. Mol. Sci. 21 (2020) 4769, https://doi.org/10.3390/ijms21134769.

[26] P.L. Uniyal, H. Govindapyari, P. Gupta, Adaptive strategies of bryophytes, in: P. Singh (Ed.), Biodiversity, Conservation and Systematics, Scientific Publishers, India, 2007, pp. 67–91.

[27] W. Kettum, C. Samart, N. Chanlek, P. Pakawanit, P. Reubroycharoen, G. Guan, .S. Kiatkamjornwong, Enhanced adsorptive composite foams for copper (II) removal utilising bio-renewable polyisoprene-functionalised carbon derived from coconut shell waste, Sci. Rep. 11 (1) (2021) 1459, https://doi.org/10.1038/s41598-020-80789-x.

[28] M.E. Mahmoud, G.M. Nabil, M.M. Zaki, M.M. Saleh, Starch functionalization of iron oxide by-product from steel industry as a sustainable low cost nanocomposite for removal of divalent toxic metal ions from water, Int. J. Biol. Macromol. 137 (2019) 455–468, https://doi.org/10.1016/j.ijbiomac.2019.06.170.

[29] M.E. Mahmoud, M.M. Osman, H. Abdel-Aal, G.M. Nabil, Microwave-assisted adsorption of Cr(VI), Cd(II) and Pb(II) in presence of magnetic graphene oxide-covalently functionalized-tryptophan nanocomposite, J. Alloys Compd. 823 (2020) 153855, https://doi.org/10.1016/j.jallcom.2020.153855.

[30] M.E. Mahmoud, M.M. Saleh, M.M. Zaki, G.M. Nabil, A sustainable nanocomposite for removal of heavy metals from water based on crosslinked sodium alginate with iron oxide waste material from steel industry, J. Environ. Chem. Eng. 8 (4) (2020) 104015, https://doi.org/10.1016/j.jece.2020.104015.

[31] US EPA, Common Chemicals Found at Superfund Sites [cited 2024 May 5], Database: US Government Printing Office, Washington, DC, 1992. EPA 540/R-94/044. Available from: https://nepis.epa.gov/Exe/ZyPDF.cgi/10002383.PDF?Dockey=10002383.PDF.

[32] D.C. Adriano, Trace Elements in Terrestrial Environments: Biogeochemistry, Bioavailability, and Risks of Metals, 860, Springer, New York, USA, 2001.

[33] C. Appel, L.Q. Ma, R.D. Rhue, W. Reve, Sequential sorption of lead and cadmium in three tropical soils, Environ. Pollut. 155 (1) (2008) 132–140, https://doi.org/10.1016/j.envpol.2007.10.026.

[34] X. Chen, M.F. Hossain, C. Duan, J. Lu, Y.F. Tsang, M.S. Islam, Y. Zhou, Isotherm models for adsorption of heavy metals from water - a review, Chemosphere 307 (Pt 1) (2022) 135545, https://doi.org/10.1016/j.chemosphere.2022.135545.

[35] M.M. Areco, L. Saleh-Medina, M.A. Trinelli, J.L. Marco-Brown, M. dos Santos Afonso, Adsorption of Cu (II), Zn (II), Cd (II) and Pb (II) by dead Avena fatua biomass and the effect of these metals on their growth, Colloids Surf. B Biointerfaces 110 (2013) 305–312.

[36] C. Phaenark, P. Harn-asa, P. Paejaroen, S. Chunchob, W. Sawangproh, Removal of Pb(II) and Cd(II) by biomass derived from broadleaf cattail and water hyacinth, J. Water Environ. Technol. 21 (2023) 191–203, https://doi.org/10.2965/jwet.22-138.

[37] N.A. Abdul Salim, M.H. Puteh, A.R.M. Yusoff, N.H. Abdullah, M.A. Fulazzaky, M.A.Z.R. Arman, M.H. Khamidun, M.A.A. Zaini, A. Syafiuddin, N. Ahmad, Z. M. Lazim, M. Nuid, N.A. Zainuddin, Adsorption isotherms and kinetics of phosphate on waste mussel shell, Mal. J. Fund. Appl. Sci. 16 (2020) 393–399, https://doi.org/10.11113/mjfas.v16n3.1752.

[38] N. Ayawei, A.N. Ebelegi, D. Wankasi, Modelling and interpretation of adsorption isotherms, J. Chem. 2017 (2017) 1–11, https://doi.org/10.1155/2017/3039817.

[39] L.B.L. Lim, N. Priyantha, H.H. Cheng, N.A. Hazirah, *Parkia speciosa* (Petai) pod as a potential low-cost adsorbent for the removal of toxic crystal violet dye, Scientia Bruneiana 15 (2016) 99–106, https://doi.org/10.46537/scibru.v15i0.26.

[40] J. Febrianto, A.N. Kosasih, J. Sunarso, Y.H. Ju, N. Indraswati, S. Ismadji, Equilibrium and kinetic studies in adsorption of heavy metals using biosorbent: a summary of recent studies, J. Hazard Mater. 162 (2009) 616–645, https://doi.org/10.1016/j.jhazmat.2008.06.042.

[41] G. Bayramoglu, S. Burcu Angi, I. Acikgoz-Erkaya, M. Yakup Arica, Preparation of effective green sorbents using *O. princeps* alga biomass with different composition of amine groups: comparison to adsorption performances for removal of a model acid dye, J. Mol. Liq. 347 (2022) 118375, https://doi.org/10.1016/j.molliq.2021.118375.

[42] F.Y. Wang, H. Wang, J.W. Ma, Adsorption of cadmium (II) ions from aqueous solution by a new low-cost adsorbent-bamboo charcoal, J. Hazard Mater. 177 (2010) 300–306, https://doi.org/10.1016/j.jhazmat.2009.12.032.

[43] F.S. Abbas, Dyes removal from wastewater using agricultural waste, Adv. Environ. Biol. 7 (2013) 1019–1026.

[44] Y.C. Lee, S.P. Chang, The biosorption of heavy metals from aqueous solution by *Spirogyra* and *Cladophora* filamentous macroalgae, Bioresour. Technol. 102 (2011) 5297–5304, https://doi.org/10.1016/j.biortech.2010.12.103.

[45] X. Ma, W. Cui, L. Yang, Y. Yang, H. Chen, K. Wang, Efficient biosorption of lead(II) and cadmium(II) ions from aqueous solutions by functionalized cell with intracellular $CaCO_3$ mineral scaffolds, Bioresour. Technol. 185 (2015) 70–78, https://doi.org/10.1016/j.biortech.2015.02.074.

[46] A. Saglam, Y. Yalcinkaya, A. Denizli, M.Y. Arica, Ö. Genc, S. Bektas, Biosorption of mercury by carboxymethylcellulose and immobilized *Phanerochaete chrysosporium*, Microchem. J. 71 (2002) 73–81, https://doi.org/10.1016/S0026-265X(01)00142-4.

[47] T. Fan, Y. Liu, B. Feng, G. Zeng, C. Yang, M. Zhou, H. Zhou, Z. Tan, X. Wang, Biosorption of cadmium(II), zinc(II) and lead(II) by *Penicillium simplicissimum*: isotherms, kinetics and thermodynamics, J. Hazard Mater. 160 (2008) 655–661, https://doi.org/10.1016/j.jhazmat.2008.03.038.

[48] M.A. Al-Ghouti, D.A. Da'ana, Guidelines for the use and interpretation of adsorption isotherm models: a review, J. Hazard Mater. 393 (2020) 122383, https://doi.org/10.1016/j.jhazmat.2020.122383.

[49] S.Y. Elovich, O.G. Larinov, Theory of adsorption from solutions of non electrolytes on solid (I) equation adsorption from solutions and the analysis of its simplest form,(II) verification of the equation of adsorption isotherm from solutions, Izvestiya Akademii Nauk. SSSR, Otdelenie Khimicheskikh Nauk 2 (2) (1962) 209–216.

[50] C. Tsamo, A. Paltahe, D. Fotio, T.A. Vincent, W.F. Sales, One-, two-, and three-parameter isotherms, kinetics, and thermodynamic evaluation of Co(II) removal from aqueous solution using dead neem leaves, Int. J. Chem. Eng. 2019 (2019) 1–14, https://doi.org/10.1155/2019/6452672.

[51] R. Sips, The structure of a catalyst surface, J. Chem. Phys. 16 (1948) 490–495, https://doi.org/10.1063/1.1746922.

[52] J. Wang, X. Guo, Adsorption isotherm models: classification, physical meaning, application and solving method, Chemosphere 258 (2020) 127279, https://doi.org/10.1016/j.chemosphere.2020.127279.

[53] M.M. Rao, G.C. Rao, K. Seshaiah, N.V. Choudary, M.C. Wang, Activated carbon from *Ceiba pentandra* hulls, an agricultural waste, as an adsorbent in the removal of lead and zinc from aqueous solutions, Waste Manag. 28 (2008) 849–858, https://doi.org/10.1016/j.wasman.2007.01.017.

[54] K. Beaugelin-Seiller, J.P. Baudin, C. Casellas, Experimental study of the effects of various factors on the uptake of ^{60}Co by freshwater mosses, Arch. Environ. Contam. Toxicol. 28 (1995) 125–133, 10.1007/bf00213977.

[55] M. Pipíška, M. Horník, L. Vrtoch, J. Augustín, J. Lesný, Biosorption of Zn and Co ions by *Evernia prunastri* from single and binary metal solutions, Chem. Ecol. 24 (2008) 181–190, https://doi.org/10.1080/02757540802069498.

[56] B. Volesky, Biosorption process simulation tools, Hydrometallurgy 71 (2003) 179–190, https://doi.org/10.1016/s0304-386x(03)00155-5.

[57] R.J. Martins, R. Pardo, R.A. Boaventura, Cadmium(II) and zinc(II) adsorption by the aquatic moss *Fontinalis antipyretica*: effect of temperature, pH and water hardness, Water Res. 38 (2004) 693–699, https://doi.org/10.1016/j.watres.2003.10.013.

[58] S. Bang, S.W. Lee, J.Y. Kim, D.L. Yu, Y.K. Kang, K.W. Kim, Adsorption of cadmium, copper, and lead on *Sphagnum* peat moss, Econ. Environ. Geol. 39 (2006) 103–109.
[59] L. Bulgariu, M. Ratoi, D. Bulgariu, M. Macoveanu, Equilibrium study of Pb(II) and Hg(II) sorption from aqueous solutions by moss peat, Environ. Eng. Manag. J. 7 (2008) 511–516, https://doi.org/10.30638/eemj.2008.073.
[60] R.J.E. Martins, V.J.R. Vilar, R.A.R. Boaventura, Kinetic modelling of cadmium and lead removal by aquatic mosses, Braz. J. Chem. Eng. 31 (2014) 229–242, https://doi.org/10.1590/S0104-66322014000100021.
[61] S.J. Lee, J.H. Park, Y.T. Ahn, J.W. Chung, Comparison of heavy metal adsorption by peat moss and peat moss-derived biochar produced under different carbonization conditions, Water Air Soil Pollut. 226 (2015), https://doi.org/10.1007/s11270-014-2275-4.
[62] A. Šuňovská, V. Hasíková, M. Horník, M. Pipíška, S. Hostin, J. Lesný, Removal of Cd by dried biomass of freshwater moss *Vesicularia dubyana*: batch and column studies, Desalin. Water Treat. 57 (2015) 2657–2668, https://doi.org/10.1080/19443994.2015.1026281.
[63] C.P. Okoli, P.N. Diagboya, I.O. Anigbogu, B.I. Olu-Owolabi, K.O. Adebowale, Competitive biosorption of Pb(II) and Cd(II) ions from aqueous solutions using chemically modified moss biomass (*Barbula lambarenensis*), Environ. Earth Sci. 76 (2016), https://doi.org/10.1007/s12665-016-6368-9.
[64] A. Di Palma, A.G. Gonzalez, P. Adamo, S. Giordano, R. Reski, O.S. Pokrovsky, Biosurface properties and lead adsorption in a clone of *Sphagnum palustre* (Mosses): towards a unified protocol of biomonitoring of airborne heavy metal pollution, Chemosphere 236 (2019) 124375, https://doi.org/10.1016/j.chemosphere.2019.124375.
[65] G.S. Manoj, G.M. Greeshma, R. Krishnan, K. Murugan, Bryophytes: a myriad hue of bio-resources with therapeutic potentialities, in: K. Arundachalam, X. Yang, S.P. Sasidharan (Eds.), Natural Product Experiments in Drug Discovery, Springer, New York, USA, 2022, pp. 321–360, https://doi.org/10.1007/978-1-0716-2683-2_21.
[66] J.M. Lezcano, F. González, A. Ballester, M.L. Blázquez, J.A. Muñoz, C. García-Balboa, Biosorption of Cd(II), Cu(II), Ni(II), Pb(II) and Zn(II) using different residual biomass, Chem. Ecol. 26 (2010) 1–17, https://doi.org/10.1080/02757540903468102.
[67] Z. Cao, Z. Wang, Z. Shang, J. Zhao, Classification and identification of *Rhodobryum roseum* Limpr. and its adulterants based on fourier-transform infrared spectroscopy (FTIR) and chemometrics, PLoS One 12 (2017) e0172359, https://doi.org/10.1371/journal.pone.0172359.
[68] A. Sari, M. Tuzen, Removal of mercury(II) from aqueous solution using moss (*Drepanocladus revolvens*) biomass: equilibrium, thermodynamic and kinetic studies, J. Hazard Mater. 171 (2009) 500–507, https://doi.org/10.1016/j.jhazmat.2009.06.023.
[69] A. Grimm, R. Zanzi, E. Björnbom, A.L. Cukierman, Comparison of different types of biomasses for copper biosorption, Bioresour. Technol. 99 (2008) 2559–2565, https://doi.org/10.1016/j.biortech.2007.04.036.
[70] A. Sari, D. Mendil, M. Tuzen, M. Soylak, Biosorption of Cd (II) and Cr (III) from aqueous solution by moss (*Hylocomium splendens*) biomass: equilibrium, kinetic and thermodynamic studies, Chem. Eng. J. 144 (2008) 1–9, https://doi.org/10.1016/j.cej.2007.12.020.
[71] A. Sari, D. Mendil, M. Tuzen, M. Soylak, Biosorption of palladium(II) from aqueous solution by moss (*Racomitrium lanuginosum*) biomass: equilibrium, kinetic and thermodynamic studies, J. Hazard Mater. 162 (2009) 874–879, https://doi.org/10.1016/j.jhazmat.2008.05.112.
[72] J. Marešová, M. Pipíška, M. Rozložník, M. Horník, L. Remenárová, J. Augustín, Cobalt and strontium sorption by moss biosorbent: modeling of single and binary metal systems, Desalination 266 (2011) 134–141, https://doi.org/10.1016/j.desal.2010.08.014.
[73] P.X. Sheng, Y.P. Ting, J.P. Chen, Biosorption of heavy metal ions (Pb, Cu, and Cd) from aqueous solutions by the marine alga *Sargassum* sp. in single-and multiple-metal systems, Ind. Eng. Chem. Res. 46 (2007) 2438–2444, https://doi.org/10.1021/ie0615786.
[74] M. Iqbal, A. Saeed, S.I. Zafar, FTIR spectrophotometry, kinetics and adsorption isotherms modeling, ion exchange, and EDX analysis for understanding the mechanism of Cd^{2+} and Pb^{2+} removal by mango peel waste, J. Hazard Mater. 164 (2009) 161–171, https://doi.org/10.1016/j.jhazmat.2008.07.141.